

# On breaking the age-metallicity degeneracy in early-type galaxies: infall versus star formation efficiency

Ignacio Ferreras and Joseph Silk\*

*Physics Dept. Denys Wilkinson Building, Keble Road, Oxford OX1 3RH*

Draft version 31 December 2013

## ABSTRACT

The correlation between  $[\text{Mg}/\text{Fe}]$  and galaxy mass found in elliptical galaxies sets a strong constraint on the duration of star formation. Furthermore, the colour-magnitude relation restricts the range of ages and metallicities of the stellar populations. We combine these two constraints with a model of star formation and chemical enrichment including infall and outflow of gas to find that the trend towards supersolar  $[\text{Mg}/\text{Fe}]$  in massive ellipticals excludes a pure metallicity sequence as an explanation of the colour-magnitude relation. An age spread is required, attributable either to a range of star formation efficiencies ( $C_{\text{eff}}$ ) or to a range of infall timescales ( $\tau_f$ ). We find that the inferred range of stellar ages is compatible with the small scatter and the redshift evolution of the colour-magnitude relation. Two alternative scenarios can explain the data: a fixed  $\tau_f$  with a mass-dependent efficiency:  $C_{\text{eff}} \propto M$ , or a fixed  $C_{\text{eff}}$  with mass-dependent infall:  $\tau_f \propto 1/\sqrt{M}$ . We conclude that the actual scenario may well involve a combination of these two parameters, with mass dependencies which should span the range of those given above.

**Key words:** galaxies: abundances — galaxies: evolution — galaxies: formation — galaxies: stellar content — galaxies: elliptical and lenticular, cD.

## 1 INTRODUCTION

In the ongoing quest for the Holy Grail of galaxy formation, suitable observables are sought to uniquely and unambiguously determine the star formation history of galaxies. Integrated broadband photometry targeting special regions of the spectral energy distribution such as the 4000Å break allows us to make a very good initial guess. The colour-magnitude relation observed in early-type galaxies (Faber 1973; Terlevich, Caldwell & Bower 2001) and its passive evolution with redshift (Stanford, Eisenhardt & Dickison 1998) is an example. The observed colours are compatible with very old stellar populations with a correlation between metallicity and galaxy mass which can be motivated by supernova-driven winds whose efficiency is modulated by the gravitational potential well (Larson 1974; Dekel & Silk 1986; Arimoto & Yoshii 1987; Matteucci & Tornambé 1987). However, the conclusions that can be drawn from integrated colours alone are blurred by the age-metallicity degeneracy (Worthey 1994). The effect of this degeneracy on the estimates of stellar ages was analyzed by Ferreras, Charlot & Silk (1999). By using the photometry of a sample of clusters over a wide redshift range ( $z \lesssim 1$ ), they found that significant late star formation – especially in intermediate and low-mass elliptical galaxies – is compatible with the data.

The failure of broadband photometry as an accurate indicator of the star formation history has directed attention towards nar-

rower spectral windows that could help to break the degeneracy. A combined analysis of Balmer and iron spectral indices from the Lick/IDS system (Worthey et al. 1994) allows us to disentangle age and metallicity. Balmer absorption is strong in main sequence A-type stars so that this index is especially sensitive to stars formed in the previous 1 – 2 Gyr of the galaxy history. This method quickly loses accuracy when older populations are considered. Furthermore, there are several contaminants to estimates of Balmer absorption such as the contribution from old stars with very low-metallicities (Maraston & Thomas 2000) as well as from small episodes of recent star formation (“frosting”; Trager et al. 2000b) which may introduce significant offsets between the observed (luminosity-weighted) and the more theoretically appealing mass-weighted ages.

In addition to the colour-magnitude relation which results in a scaling between mass and  $[\text{Fe}/\text{H}]$ , elliptical galaxies display a correlation between  $[\text{Mg}/\text{Fe}]$  and galaxy mass, so that massive early-type galaxies are enhanced with respect to the predictions from population synthesis models with solar abundance ratios (Worthey, Faber & González 1992; Davies, Sadler & Peletier 1993; Kuntscher 2000; Trager et al. 2000a). The main contributors of magnesium and iron to the ISM: type II and type Ia supernovae, respectively, take place on remarkably different timescales (e.g. Matteucci & Recchi 2001). Hence,  $[\text{Mg}/\text{Fe}]$  represents a valuable tool to measure star formation timescales. Thomas, Greggio & Bender (1999) explored this correlation to find that formation timescales should not exceed 1 Gyr. Furthermore,  $[\text{Mg}/\text{Fe}]$  measurements pose strong

\* ferreras,silk@astro.ox.ac.uk

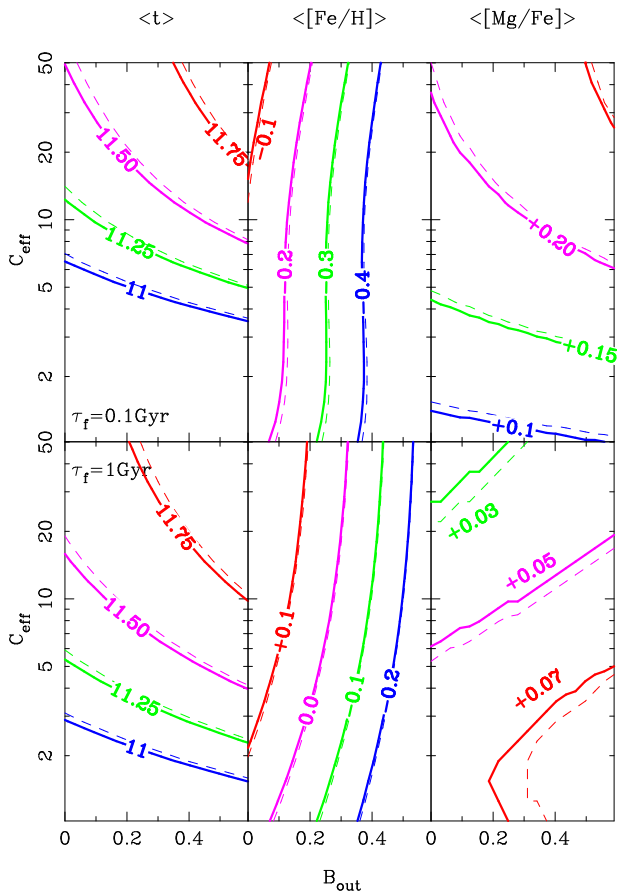


**Figure 1.** Mass-weighted averages of stellar age (*left*), metallicity (*center*), and  $[\text{Mg}/\text{Fe}]$  (*right*), for a model with fixed formation epoch ( $z_F = 3$ ) and for two different infall timescales:  $\tau_f = 0.1$  Gyr (*top*) and  $0.5$  Gyr (*bottom*). The model is explored as a function of star formation efficiency ( $C_{\text{eff}}$ ) and outflow fraction ( $B_{\text{out}}$ ). The solid (dashed) contours are mass- (luminosity-) weighted values. Notice the observed range of  $[\text{Mg}/\text{Fe}]$  cannot be reproduced by the model with a longer infall timescale (*bottom*). The correlations of both  $[\text{Fe}/\text{H}]$  and  $[\text{Mg}/\text{Fe}]$  with mass observed in elliptical galaxies can be explained by either a range of efficiencies or by a mixed  $C_{\text{eff}} + B_{\text{out}}$  sequence. Notice that massive ellipticals require a non-negligible outflow fraction. A  $B_{\text{out}}$  sequence (which translates into a pure metallicity sequence) is ruled out by the  $[\text{Mg}/\text{Fe}]$ -mass correlation.

constraints on hierarchical clustering models, so that the baryon physics controlling star formation in galaxies must be significantly decoupled from the evolution of their dark matter halos.

The purpose of this paper is to make a combined analysis of broadband photometry (which is most sensitive to age and metallicity) and the  $[\text{Mg}/\text{Fe}]$  abundance ratio (which is sensitive to the duration of the bursting stages) in order to constrain the star formation history. One aspect is crucial to this paper: to determine the possible correlation of the various parameters that control star formation with a global property of the galaxy such as its total mass. We focus on infall and outflow rates as well as on the star formation efficiency. A previous analysis using broadband photometry Ferreras & Silk (2000, paper I) concluded that there was still a degeneracy so that both outflow rates and star formation efficiencies could scale with galaxy mass. In this paper, we show that the addition of  $[\text{Mg}/\text{Fe}]$  to the analysis enables us to constrain the parameter space, ruling out pure metallicity sequences, and allowing either the

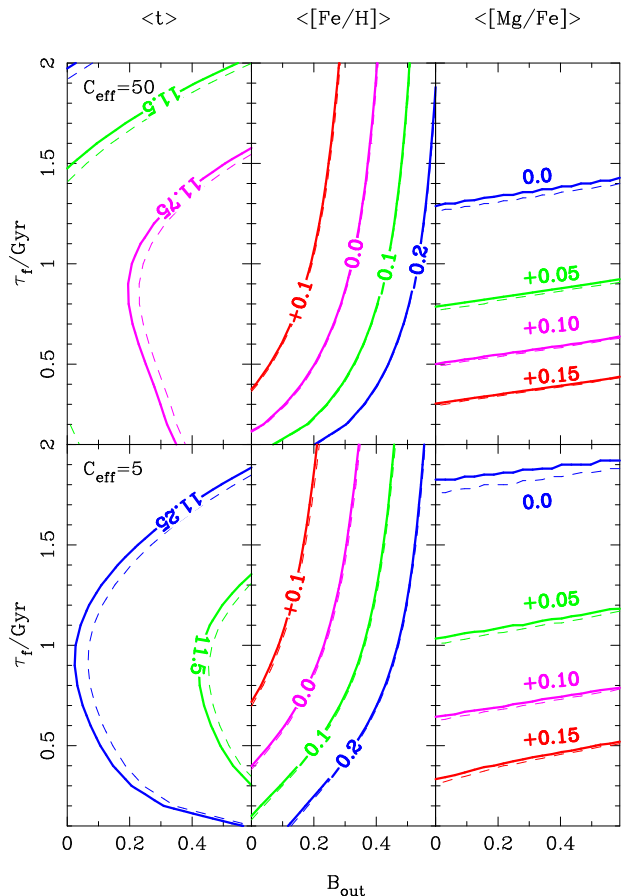


**Figure 2.** Same as figure 1 for a range of infall timescales ( $\tau_f$ ) and outflow gas fraction ( $B_{\text{out}}$ ) for two star formation efficiencies:  $C_{\text{eff}} = 100$  (*top*) and  $10$  (*bottom*). In this case, no trajectory in the ( $\tau_f, B_{\text{out}}$ ) can be found that explains *both* trends of  $[\text{Fe}/\text{H}]$  and  $[\text{Mg}/\text{Fe}]$  with galaxy mass. This implies star formation efficiency and outflows are the parameters strongly dependent on mass, whereas infall timescale should have a weaker dependence.

star formation efficiency or the infall timescale to depend on galaxy mass.

## 2 A SIMPLE MODEL OF STAR FORMATION

We explore a one-zone model of star formation and chemical enrichment as described in Ferreras & Silk (2000). Each star formation history is determined by a set of four parameters: star formation efficiency ( $C_{\text{eff}}$ ); fraction of gas and metals ejected in outflows ( $B_{\text{out}}$ ), infall timescale ( $\tau_f$ ) and formation epoch ( $z_F$ ). We model the infall rate of primordial gas by a gaussian function whose spread is given by  $\tau_f$  and whose epoch at maximum infall rate is given by the formation redshift  $z_F$ . We assume a Salpeter IMF in the mass range  $0.1 < M/M_\odot < 60$ . The model tracks the stellar, gas and metal components. The yields from type II supernovae (SNII) are taken from Thielemann, Nomoto & Hashimoto (1996) for a range of progenitor masses. Type Ia supernovae (SNIa) are included using the prescription of Greggio & Renzini (1983) assuming a close binary composed of a white dwarf and a non-degenerate companion in the (binary) mass range  $3 - 16 M_\odot$ . We refer the reader to Matteucci & Recchi (2001) for a comprehensive review of estimates of SNIa rates. The yields are taken from model

W7 in Iwamoto et al. (1999). Two elements are considered in this paper: magnesium and iron. The production of these two elements is remarkably different between both supernova types. A very significant amount of iron is produced in SNIa with respect to the  $\alpha$  elements such as Mg. The mass contained in O-, Ne- and C-burning shells is too small compared with the mass in the Si-burning zone. This implies SNIa ejecta are dominated by the products of complete and incomplete Si-burning, i.e. a higher iron yield compared to the ejecta from core-collapse (type II) supernovae. Most of the iron produced in the latter falls inside a mass-cut that collapses to form the stellar remnant. Furthermore, the different timescale for the onset of both supernova types makes abundance ratios such as  $[\text{Mg}/\text{Fe}]$  very sensitive tracers of the duration of star formation. Short-lived and intense bursts of star formation generate stellar populations mainly polluted by the elements contributed by SNIa, resulting in enhanced  $[\text{Mg}/\text{Fe}]$ . On the other hand, a more extended and weaker star formation history will allow the iron produced in SNIa's to contribute significantly to the stellar metallicity, lowering the  $[\text{Mg}/\text{Fe}]$  ratio.

Hence, there is a direct – albeit non-trivial – correspondence between  $[\text{Mg}/\text{Fe}]$  and star formation duration. Similarly to analyses of metallicities performed to infer the star formation history, the absolute estimate of the lapse of star formation is highly dependent on the stellar yields used. Thomas et al. (1999) find a significant difference between estimates of the star formation timescale using the SNIa yields from Woosley & Weaver (1995) and from Thielemann, Nomoto & Hashimoto (1996). The star formation timescale could be reduced by a factor up to 100 when using the yields from the former. The models of Thielemann et al. (1996) have a higher yield of Mg for stellar masses  $M \sim 20 - 25 M_{\odot}$ . This discrepancy is claimed to be caused by the different criterion used for convection. Furthermore, the models of Woosley & Weaver (1995) generate more iron (models B,C). Most of the Mg is produced during hydrostatic burning of the carbon shell. However, the mechanism for the production of  $^{56}\text{Ni}$  which decays into  $^{56}\text{Fe}$  is strongly dependent on the highly uncertain explosion mechanism. Throughout this paper we will use the yields from Thielemann et al. (1996) for SNIa. However, more work is definitely needed in this field if we want to make accurate estimates of the star formation timescales.

### 3 INFALL VERSUS EFFICIENCY

Figure 1 shows mass- (solid) and luminosity-weighted (dashed) contours of age (*left*),  $[\text{Fe}/\text{H}]$  (*centre*), and  $[\text{Mg}/\text{Fe}]$  (*right*) as a function of star formation efficiency ( $C_{\text{eff}}$ ) and gas outflow fraction ( $B_{\text{out}}$ ) for two infall timescales:  $\tau_f = 0.1$  Gyr (*top*) and 1 Gyr (*bottom*). The formation epoch is  $z_F = 3$ , which is compatible with the best estimate of the formation redshift of the stellar populations in ellipticals from an analysis of the fundamental plane in clusters out to  $z \sim 1.3$  (Van Dokkum & Stanford 2002). Short infall timescales are required if we want to reproduce the observed range of abundance ratios (e.g. Trager et al. 2000a; Kuntschner 2000), otherwise, choosing longer timescales would imply very low star formation efficiencies ( $C_{\text{eff}} < 1$ ) in order to achieve low abundance ratios  $[\text{Mg}/\text{Fe}] \sim 0.0 - 0.05$ , and would generate young stellar populations which will not reproduce the redshift evolution of the observed slope and scatter of the colour-magnitude relation (Stanford et al. 1998). The parameter range shown in figures 1 and 2 is chosen to avoid such young stellar populations. The birthrate parameter —  $b \equiv \psi/\langle\psi\rangle$  — for all models considered in this paper is below  $b \lesssim 0.05$ , i.e. the models never reach the lowest birthrates

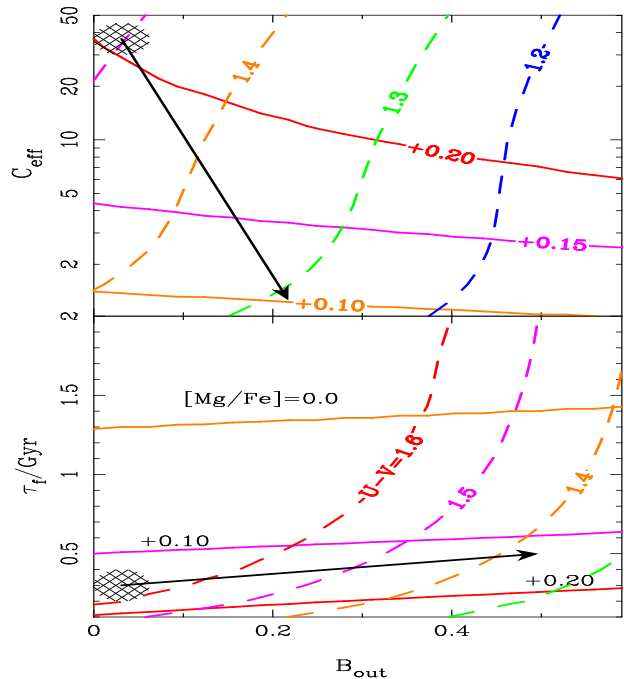


**Figure 3.** A comparison of two alternative scenarios: the colours and abundance ratios observed in early-type galaxies can be explained by a correlation between mass and either star formation efficiencies (*top*) or infall timescales (*bottom*). The thick contours give  $[\text{Mg}/\text{Fe}]$  abundance ratios. The prediction for a simple stellar population with the age and metallicity determined by the model is shown by (dashed) contours of  $U - V$  colour. The arrows give a rough locus of the mass sequence, with the hatched region representing the most massive elliptical.

of early-type disks (Kennicutt, Tamblyn & Congdon 1994). The  $\tau_f = 0.1$  Gyr model shown in figure 1 shows that a  $B_{\text{out}}$  sequence (i.e. a horizontal line in the figure) – in which only the outflow fraction is assumed to vary with galaxy mass – could explain the mass-metallicity relation compatible with the colour-magnitude relation, as suggested by Kodama & Arimoto (1997). However, the constraint imposed by the correlation between  $[\text{Mg}/\text{Fe}]$  and galaxy mass excludes this as a possibility. A range of efficiencies (“ $C_{\text{eff}}$  sequence”, vertical line) or a tilted “ $C_{\text{eff}} + B_{\text{out}}$ ” sequence is needed to explain both correlations. Hence, the combined analysis of  $[\text{Mg}/\text{Fe}]$  and  $[\text{Fe}/\text{H}]$  poses very powerful constraints on the star formation history.

Figure 2 presents a similar plot to the previous figure. In this case a range of infall timescales and outflow fractions are explored. Two star formation efficiencies are considered:  $C_{\text{eff}} = 50$  (*top*) and 5 (*bottom*). The figure shows that the range of abundance ratios could be explained by longer infall timescales in low-mass galaxies. Figures 1 and 2 illustrate the degeneracy between star formation efficiency and infall timescale, as both can reproduce a similar range of star formation histories. However, the chemical enrichment can be used to break this degeneracy, as seen in the central panel of figure 2. Models with long infall timescales give solar  $[\text{Mg}/\text{Fe}]$  but they also predict higher  $[\text{Fe}/\text{H}]$ . Hence, an explanation of the observed correlation between colour and  $[\text{Mg}/\text{Fe}]$  requires much larger outflow fractions if a range of infall timescales is assumed. Figure 3 further illustrates this point by overlaying contours of  $U - V$  colour as predicted by population synthesis models (Bruzual & Charlot, in preparation) on  $[\text{Mg}/\text{Fe}]$  contours for a model with varying star formation efficiency (*top*) or in-

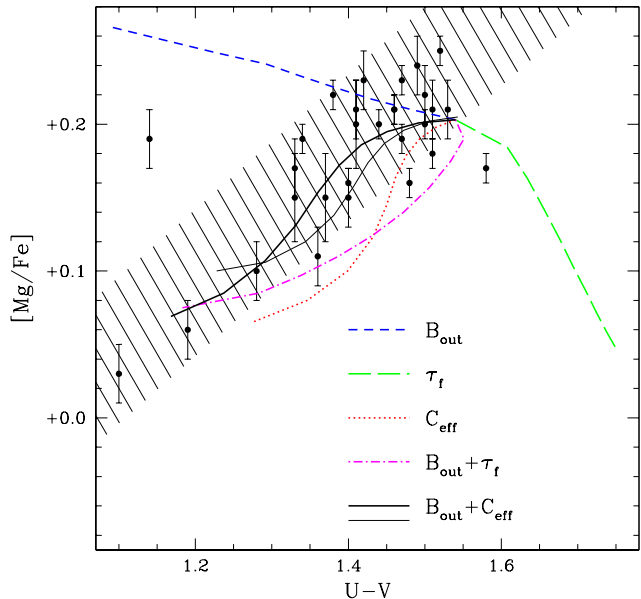


**Figure 4.** Observed correlation between  $[\text{Mg}/\text{Fe}]$  and  $U - V$  colour from the sample of González (1993) later analyzed by Trager et al. (2000a). Several model predictions are shown as discussed in the text. The shaded region is a fit to the data and is used to determine the parameters shown in figure 5.

fall timescale (*bottom*). The hatched regions represent the area of parameter space that best explains massive ellipticals. The arrow gives the locus of points which track a sequence of galaxy masses. One can see from the figure that a remarkably larger range of outflow fractions is needed if a mass-independent star formation efficiency is assumed.

Figure 4 shows the observed correlation between  $[\text{Mg}/\text{Fe}]$  and  $U - V$  colour from the sample of González (1993), which has been analyzed in detail by Trager et al. (2000a; 2000b). The translation from the observed spectral indices to estimates of  $[\text{Mg}/\text{Fe}]$  is performed by correcting the population synthesis models calibrated for solar abundance ratios using the model atmospheres for non-solar ratios of a 5 Gyr isochrone studied by Tripicco & Bell (1995). This introduces a systematic error which prevents us from getting accurate estimates of the absolute value of  $[\text{Mg}/\text{Fe}]$ . However, the relative values are more robust and the data shown in the figure gives a clear sign of a correlation between metallicity and star formation timescale. The lines give the model predictions when some of the parameters are kept constant. The dashed line is the prediction for a constant efficiency and infall timescale, so that only the outflow fraction –  $B_{\text{out}}$  – is allowed to vary with galaxy mass. This model is incompatible with the data as  $[\text{Mg}/\text{Fe}]$  is predicted to increase towards blue  $U - V$  colour. The model with a varying infall timescale and constant  $C_{\text{eff}}$  and  $B_{\text{out}}$  (long dashed line) is also ruled out as redder colours are predicted with decreasing  $[\text{Mg}/\text{Fe}]$ . The other three models are – within model and observational uncertainties – compatible with the data, although the one which seems to give a best fit to the data is the model with a constant infall timescale and a varying  $C_{\text{eff}}$  and  $B_{\text{out}}$  (solid line). The shaded area shown in figure 4 represents the best fit to the data points along with a  $\pm 0.05$  dex scatter:

$$[\text{Mg}/\text{Fe}] = 0.46(U - V) - 0.46 \pm 0.05. \quad (1)$$

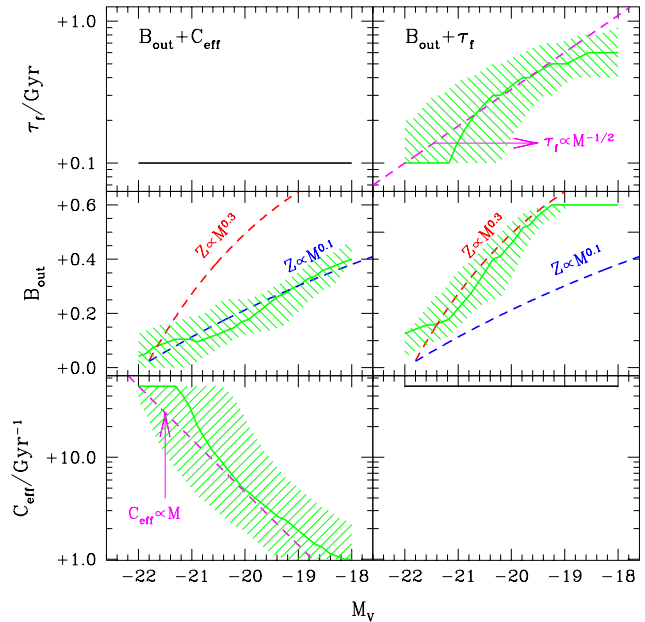


**Figure 5.** Correlation of the model parameters with the  $V$ -band absolute luminosity, using the observed  $U - V$  and  $[\text{Mg}/\text{Fe}]$  correlation with  $M_V$  as constraints. The left and right panels represent a model with constant star formation efficiency or infall timescale, respectively. The shaded regions in each panel are mappings of the region shown in figure 4 for each parameter. The solid lines give the mapping of the best fit. The dashed lines are some “educated guesses” for the mass dependence of these parameters.

Figure 5 shows the mapping of this region in parameter space for the two most plausible scenarios, namely for a fixed infall timescale (“ $B_{\text{out}} + C_{\text{eff}}$  sequence”, *left*) or for a fixed star formation efficiency (“ $B_{\text{out}} + \tau_f$  sequence”, *right*). The  $U - V$  colour-magnitude relation of the Coma cluster is used in order to translate between colour and absolute luminosity (Terlevich et al. 2001). A fixed star formation efficiency requires low-mass galaxies ( $M_V > -19$ ) to have extremely high outflow fractions ( $B_{\text{out}} > 0.6$ ). Models with a mass-dependent efficiency require a smaller range of outflows:  $0 < B_{\text{out}} < 0.4$ . Doubtlessly, the real scenario will involve a range of all three parameters considered:  $B_{\text{out}}$ ,  $C_{\text{eff}}$  and  $\tau_f$ . However, the colour constraint on the range of outflows makes a stronger dependence of  $C_{\text{eff}}$  on mass more plausible. The dashed lines in the panels of figure 5 are guesses for the correlation with mass, using the observed dependence of  $M/L_V$  on galaxy mass in cluster ellipticals (Mobasher et al. 1999). The infall model (*top right*) gives a good fit to a  $\tau_f \propto 1/\sqrt{M}$  scaling, which can be theoretically motivated if we write the accretion timescale as the cross-section per unit mass:

$$\tau_f \sim \frac{R^2}{M} \sim \frac{1}{M^{1/3} \rho^{2/3}}. \quad (2)$$

If we assume a small range of formation redshifts, the correlation between  $\tau_f$  and mass is compatible with the model predictions shown in the top right panel of figure 5. On the other hand, the efficiency model (*bottom left*) favours a linear correlation with mass:  $C_{\text{eff}} \propto M$ , a result which can be theoretically motivated by the effects of feedback on star formation (Silk 2002). The dashed lines in the middle panels span the plausible range of the correlation between mass and metallicity:  $1 - B_{\text{out}} \propto \langle Z \rangle \propto M^\alpha$ , with

$\alpha \sim 0.3 - 0.1$  (e.g. Larson 1974; Mould 1984; Dekel & Silk 1986). Hence, a shallow mass-metallicity relation ( $\alpha \sim 0.1$ ) favours a model with a mass-dependent star formation efficiency, whereas infall timescales should be more dependent on the mass of the galaxy if  $\alpha \sim 0.3$ . All these correlations are nevertheless strongly model-dependent, so that we could expect the real mechanism to lie in between these two alternative scenarios, i.e. the efficiency should be at most linearly dependent on mass and the infall timescale should at most vary as  $1/\sqrt{M}$ .

#### 4 CONCLUSIONS

We have explored the correlation between  $U - V$  colour and  $[\text{Mg}/\text{Fe}]$  in early-type galaxies to determine the role of the galaxy mass in the formation of this type of galaxies. Infall timescale ( $\tau_f$ ), star formation efficiency ( $C_{\text{eff}}$ ) and gas outflows ( $B_{\text{out}}$ ) are the main “drivers” for this correlation. The formation epoch is kept fixed throughout the paper to  $z_F = 3$ . This is motivated by the fact that  $z_F$  is tightly constrained by the observed evolution of the fundamental plane or the colour-magnitude relation in clusters out to  $z \lesssim 1.3$  (Stanford et al. 1998; Van Dokkum & Stanford 2002), so that values  $z_F \lesssim 2$  are readily ruled out. Earlier formation epochs do not significantly change the results shown in this paper. In the list of caveats that any model of chemical enrichment always carries, we should emphasize the strong dependence of the model predictions on the stellar yields. In this paper we have made use of the models of Thielemann et al. (1996) for type II SNe and of Iwamoto et al. (1999) for type Ia SNe. The currently available alternative for type II SNe yields, namely Woosley & Weaver (1995), gives similar metallicities, but rather low  $[\text{Mg}/\text{Fe}]$  abundance ratios unless extremely short infall timescales are considered (Thomas et al. 1999).

Pre-enrichment of the infalling gas is a mechanism which could alter the model predictions. However, as long as we assume the abundance ratios of the pre-enriched gas to be similar to type II SNe ejecta, our model gives higher metallicities and roughly similar  $[\text{Mg}/\text{Fe}]$ . Hence, a slight increase in  $B_{\text{out}}$  lowers  $[\text{Fe}/\text{H}]$  enough to give equally good fits to the data. The solid lines in figure 4 are “ $B_{\text{out}} + C_{\text{eff}}$ ” sequences with the infalling gas having zero metallicity (thick line) or  $Z_{\odot}/10$  with enhanced  $[\text{Mg}/\text{Fe}] = +0.3$  dex (thin line). The difference between these two is negligible within the underlying uncertainties. This illustrates the fact that absolute estimates of parameters in chemical enrichment models are prone to large systematic errors. Nevertheless, the relative estimates are robust and only weakly dependent on these uncertainties.

Figures 1 and 2 show that the  $[\text{Mg}/\text{Fe}]$  data poses a degeneracy between infall timescale and star formation efficiency, which is to be expected since the data can only constrain the duration of the star formation episode. The constraint on the metallicity from the colour-magnitude relation is added to the analysis, so that this degeneracy is partially lifted. The model shows that a mass-dependent range of outflow fractions is required to explain both  $U - V$  and  $[\text{Mg}/\text{Fe}]$ . Furthermore, a simple model in which *only*  $B_{\text{out}}$  scales with mass is incompatible with the data. Hence, a pure metallicity sequence is readily ruled out by the observations. A certain spread in the ages is thereby expected in ellipticals, although the predicted range of ages is for all practical purposes indistinguishable from a fixed age population in local and moderate redshift ellipticals. The range of infall timescales or star formation efficiencies has been shown to be degenerate, although figure 4 might favour a scenario in which the efficiency has a strong dependence on galaxy mass,

of order:  $C_{\text{eff}} \propto M$ . Nevertheless, a range of infall timescales  $\tau_f \propto 1/\sqrt{M}$  is also compatible with the data and the assumption of a mass-metallicity relation  $Z \propto M^{0.3-0.1}$  favours this model. The accurate measurement of the mass-metallicity relation will be one of the key observables for disentangling infall timescales and star formation efficiency.

#### REFERENCES

- Arimoto, N. & Yoshii, Y., 1987, *A&A*, 173, 23  
 Davies, R. L., Sadler, E. M. & Peletier, R., 1993, *MNRAS*, 262, 650  
 Dekel, A. & Silk, J., 1986, *ApJ*, 303, 39  
 Faber, S. M., 1973, *ApJ*, 179, 731  
 Ferreras, I., Charlot, S. & Silk, J., 1999, *ApJ*, 521, 81  
 Ferreras, I. & Silk, J., 2000, *MNRAS*, 316, 786 (Paper I)  
 González, J. J. Ph.D. thesis, Univ. California, Santa Cruz.  
 Iwamoto, K., Brachwitz, F., Nomoto, K., Kishimoto, N., Umeda, H., Hix, W. R., Thielemann, F.-K., 1999, *ApJS*, 125, 439  
 Kennicutt, R. C., Tamblyn, P. & Congdon, C. W., 1994, *ApJ*, 435, 22  
 Kodama, T. & Arimoto, N. 1997, *A&A*, 320, 41  
 Kuntschner, H. 2000, *MNRAS*, 315, 184  
 Larson, R. B., 1974, *MNRAS*, 169, 229  
 Maraston, C. & Thomas, D. 2000, *ApJ*, 541, 126  
 Matteucci, F. & Tornambé, A., 1987, *A&A*, 185, 51  
 Matteucci, F. & Recchi, S. 2001, *ApJ*, 558, 351  
 Mobasher, B., Guzmán, R., Aragón-Salamanca, A. & Zepf, S., 1999, *MNRAS*, 304, 225  
 Mould, J. R., 1984, *PASP*, 96, 773  
 Silk, J., 2002, *MNRAS*, submitted  
 Stanford, S. A., Eisenhardt, P. R. & Dickinson, M. 1998, *ApJ*, 492, 461  
 Terlevich, A. I., Caldwell, N. & Bower, R. G., 2001, *MNRAS*, 326, 1547  
 Thielemann, F.-K., Nomoto, K. & Hashimoto, M., 1996, *ApJ*, 460, 408  
 Thomas, D., Greggio, L. & Bender, R., 1999, *MNRAS*, 302, 537  
 Trager, S. C., Faber, S. M., Worthey, G. & González, J. J., 2000a, *AJ*, 119, 1645  
 Trager, S. C., Faber, S. M., Worthey, G. & González, J. J., 2000b, *AJ*, 120, 165  
 Tripicco, M. J. & Bell, R. A. 1995, *AJ*, 110, 3035  
 Van Dokkum, P. G. & Stanford, S. A., 2002, *ApJ*, in press, astro-ph/0210643  
 Woosley, S. E. & Weaver, T. A., 1995, *ApJS*, 101, 181  
 Worthey, G., Faber, S. M. & González, J. J., 1992, *ApJ*, 398, 73  
 Worthey, G., Faber, S. M., González, J. J. & Burstein, D. 1994, *ApJS*, 94, 687  
 Worthey, G. 1994, *ApJS*, 95, 107

This paper has been typeset from a  $\text{\TeX}/\text{\LaTeX}$  file prepared by the author.